Neuroscience 364 (2017) 60–70

SYSTEMIC ADMINISTRATION OF TWO DIFFERENT ANXIOLYTIC DRUGS DECREASES LOCAL FIELD POTENTIAL THETA FREQUENCY IN THE MEDIAL ENTORHINAL CORTEX WITHOUT AFFECTING GRID CELL FIRING FIELDS

CAITLIN K. MONAGHAN,[†]* G. WILLIAM CHAPMAN IV[‡] AND MICHAEL E. HASSELMO

Boston University, Center for Systems Neuroscience, Graduate Program for Neuroscience, Department of Psychological and Brain Sciences, 610 Commonwealth Avenue, Boston, MA 02215, USA

Abstract—Neurons coding spatial location (grid cells) are found in medial entorhinal cortex (MEC) and demonstrate increasing size of firing fields and spacing between fields (grid scale) along the dorsoventral axis. This change in grid scale correlates with differences in theta frequency, a 6–10 Hz rhythm in the local field potential (LFP) and rhythmic firing of cells. A relationship between theta frequency and grid scale can be found when examining grid cells recorded in different locations along the dorsoventral axis of MEC. When describing the relationship between theta frequency and grid scale, it is important to account for the strong positive correlation between theta frequency and running speed. Plotting LFP theta frequency across running speeds dissociates two components of this relationship: slope and intercept of the linear fit. Change in theta frequency through a change in the slope component has been modeled and shown experimentally to affect grid scale, but the prediction that change in the intercept component would not affect grid scale has not been tested experimentally. This prediction about the relationship of intercept to grid scale is the primary hypothesis tested in the experiments presented here. All known anxiolytic drugs decrease hippocampal theta frequency despite their differing mechanisms of action. Specifically, anxiolytics decrease the intercept of the theta frequency-running speed relationship in the hippocampus. Here we demonstrate that anxiolytics decrease the intercept of the theta frequency-running speed relationship in the MEC, similar to hippocampus, and the decrease in frequency through this change in intercept does not affect grid scale.

Key words: navigation, theta, grid cells, 8-OH-DPAT, diazepam.

INTRODUCTION

Grid cells are strikingly spatially modulated cells that fire action potentials in multiple but very specific locations in an environment as an animal forages for food (Fyhn et al., 2004; Hafting et al., 2005). These firing fields, or grid fields, fire in a pattern corresponding to the corners of tightly packed equilateral triangles tessellating the area traveled. These cells have been primarily recorded in the rodent medial entorhinal cortex (MEC) (Fyhn et al., 2004; Hafting et al., 2005), along with the connected regions of the pre- and parasubiculum (Boccara et al., 2010). Within these and other regions, "head direction" (HD) cells have also been reported, which fire action potentials when an animal is facing a certain direction (Taube et al., 1990; Sargolini et al., 2006). Together, these cells, along with other activity in these regions, likely contribute to an animal's sense of spatial location.

Throughout the MEC and connected regions, a prominent 6–10 Hz rhythm ("theta") appears in the local field potential (LFP) and in the rhythmic firing of single units, such as grid cells. This oscillation was first described in hippocampal LFP and single units (Green and Arduini, 1954; Vanderwolf, 1969; Bland, 1986) and subsequently reported in the MEC in both the LFP and the single unit rhythmicity as well (Mitchell and Ranck, 1980; Alonso and García-Austt, 1987). Grid cells often fire coincidentally with phases of the LFP theta rhythm when an animal traverses through individual firing fields of a grid cell. Coincidental firing can occur either consistently at the same phase of the oscillation ("phase locked") or at progressively earlier phases across successive theta cycles ("phase precessing") across each pass through the grid field area (Hafting et al., 2008; Climer et al., 2013). The maintenance of this relationship requires the adaptation of activity to running speed, in order to account for differences in the time it takes to traverse an otherwise

*Corresponding author. Address: Psychosis Neurobiology Laboratory, Mailstop 223, McLean Hospital, 115 Mill Street, Belmont, MA 02478, USA.
E-mail address: cmonaghan@mclean.harvard.edu (C. K. Monaghan).
[†] Present address: Psychotic Disorders Division, McLean Hospital, Harvard Medical School, Belmont, MA 02452, USA.
[‡] Present address: Department of Psychology and Neuroscience, Center for Neuroscience, University of Colorado Boulder, Boulder, CO 80301, USA.
Abbreviations: 5-HT, 5-hydroxytryptamine (serotonin); LFP, local field potential; MEC, medial entorhinal cortex; OIM, oscillatory interference model.

https://doi.org/10.1016/j.neuroscience.2017.08.056
0306-4522/

identical path with differences in speed. In line with this, the frequency of the theta oscillation in the LFP shows a very strong positive correlation with running speed in the MEC (Jeewajee et al., 2008a) and is correlated with grid cell properties in many other ways as well.

Grid fields increase in size and spacing (grid scale) in grid cells recorded along the dorsal to ventral axis of the MEC (Hafting et al., 2005; Sargolini et al., 2006; Brun et al., 2008), which has been linked to changes in theta frequency. This grid scale increase along the axis correlates with the period of the subthreshold membrane potential oscillation recorded in layer II MEC stellate cells *in vitro* (Giocomo et al., 2007). Furthermore, the frequency of the rhythmicity of grid cell firing is inversely correlated with increasing grid field sizes (Jeewajee et al., 2008a; Stensola et al., 2012). Grid scale also increases in response to a novel environment, while the rhythmicity of firing decreases in frequency (the oscillation period increases) (Barry et al., 2012). Consistent with the many correlations reported between grid cells and theta rhythm, theta rhythm has been utilized in many computational models of the location-related activity of grid cells.

Oscillatory interference models (OIMs) take advantage of the prominent theta rhythm to generate the spatially periodic firing of grid cells. The general principle behind these models is that two slightly different oscillations, for example found in the LFP and in a given cell's subthreshold membrane potential oscillations, produce constructive and deconstructive interference when the peaks of their oscillations align or cancel out, respectively. During times of peak alignment, this drives the given neuron to spike, producing a grid-like pattern. These models use differing oscillation frequencies to produce the different scales of grid cell firing found along the dorsoventral axis and actually predicted that the frequency of intrinsic subthreshold membrane potential oscillations decreases in cells along this axis (O'Keefe and Burgess, 2005; Giocomo et al., 2007). Importantly, the frequency of theta oscillations must increase with running speed in order to maintain consistent firing patterns regardless of velocity, matching biological data (Jeewajee et al., 2008a).

When describing theta frequency in terms of how it relates to grid scale, it is important to consider that theta frequency is very strongly correlated with running speed. Thus, taking the additional variable of running speed into account results in a more accurate and thorough depiction of how theta frequency and grid scale relate. Specifically, the relationship between theta frequency and running speed can be broken down into two dissociable components. Fitting a regression line to the values of theta frequency plotted across increasing running speeds gives both an intercept and a slope value to represent this relationship. Based on the OIM, Burgess (2008) suggested that grid field scale was not directly affected by a change in overall theta frequency, but specifically only by a change in the slope, and not the intercept, of this linear fit (Burgess, 2008). This prediction is partially supported by the findings that exposure to a novel environment increases grid scale and decreases the slope of hippocampal theta frequency plotted across running speeds (Barry et al., 2012; Wells et al., 2013). However, the prediction that a change in the intercept component of this relationship would be unable to produce similar changes in grid scale compared to those caused by a change in the slope has not been explicitly tested. This prediction about the relationship between grid scale and the intercept of the plot of theta frequency versus running speed is the hypothesis that is tested in the experiments presented here.

One hallmark of all presently known anxiolytic drugs is that they cause a robust decrease in the hippocampal theta frequency elicited via reticular formation stimulation (Coop and McNaughton, 1991; McNaughton and Coop, 1991; McNaughton et al., 2007) or during running in awake behaving animals (Wells et al., 2013). Specifically, Wells et al. (2013) demonstrated that this decrease in hippocampal theta frequency during running comes from a reduction in the intercept and not the slope component of the linear fit between theta frequency and running speed.

The study presented here examined whether systemic administration of a serotonergic anxiolytic or benzodiazepine anxiolytic reduced the intercept component of the relationship between theta frequency and running speed recorded in the MEC, similar to what was reported for these drug types in the hippocampus (Wells et al., 2013). We then tested the prediction that a change in theta frequency acting on the intercept component of the theta frequency-running speed relationship would not produce changes in grid scale, in contrast to data showing changes in grid scale associated with a change in the slope of this relationship.

EXPERIMENTAL PROCEDURES

Subjects

Male Long-Evans rats (Charles River Laboratories) weighing between 350 and 450 g at surgery were used for these studies (n = 10). All experimental procedures were approved by the Institutional Animal Care and Use Committee for the Charles River Campus at Boston University. Rats were housed individually in plexiglass cages, maintained on a 12-h light/12-h dark cycle (testing always occurred during the light cycle) and were maintained at ~85% of their ad libitum weight. Prior to surgery, rats were habituated to the experimenter and testing room. The animals were trained to forage in an open field environment (1 m by 1.5 m) for pieces of Froot Loops (Kellogg's). One wall of the otherwise black painted environment was white to provide stable landmark information; cues surrounding the environment were present to provide distal information as well.

Implant

Rats were implanted with recording drives housing up to 16 individually moveable tetrodes (four 12.7 μm nichrome wires spun together) and 4 reference tetrodes, aimed at the MEC. Tetrodes were gold plated to bring down the impedance to < 150 kOhm. The exit of the drive was angled at ~25 degrees in the posterior

direction in order to implant just anterior of the transverse sinus.

Surgery

Rats were anesthetized with isoflurane and given an injection of a ketamine/xylazine/acepromazine cocktail and buprenorphine; depth of anesthesia was monitored at least every 15 min by checking breathing and confirming lack of response to a toe pinch. An injection of atropine was given to prevent fluid buildup in the lungs. After the initial incision, the skull area was cleared of fascia, and approximately 10 holes were drilled to attach anchor screws into the skull; 1–2 ground screws were placed over the cerebellum. Two craniotomies were performed: one to implant a drug delivery cannula for use in another set of experiments (from Bregma: 0.5 mm anterior, 3.0 mm lateral; implanted at 25 degrees medially, lowered 6.0 mm from brain surface) and the second as the implant site (left hemisphere; most lateral and posterior corner grazes where the left bone ridge and lambda suture meet). The implant was secured in place using Kwik-Sil and dental acrylic. Tetrodes were lowered 2–3 mm from the dorsal surface at surgery. Animals were allowed one week to fully recover after surgery before experiments began.

Neural recordings

Animals were tested daily in the open field during recording sessions to search for grid cells, conjunctive grid-by-head-direction cells, head direction cells, border cells, and theta rhythmic cells. Once theta rhythmic cells and theta oscillations in the LFP were recorded, tetrodes were lowered a maximum of ~35 μm/day; experiments were never done on days tetrodes were turned in order to maximize the likelihood of recording the same cells across sessions on a single day. Neural signals were preamplified by unity-gain operational amplifiers located on the head of the animal. Signals were linked to digital amplifiers and amplified (5000–20,000X) and bandpass filtered (1–500 Hz) by the 64-channel Cheetah Digital Lynx acquisition system (Neuralynx Corp., Bozeman, MT). When a signal crossed threshold all four channels of the tetrode were digitized at 32 kHz and recorded. Position, head direction, and velocity data were calculated from a red (front) and green (back) diode positioned on the recording head stage and sampled at 30 Hz. Position was determined as the centroid of the diodes. LFP activity was collected at 32 kHz and downsampled to 508 Hz. LFP traces obtained from the MEC were recorded from a single lead of a tetrode and referenced to the animal ground or to a cortical electrode that did not show theta oscillations when referenced to ground.

Histology

When possible, final tetrode positions were marked before sacrificing the animal by passing current through tetrodes that had recorded grid cells, the strongest LFP theta, and the reference tetrodes used, if applicable. Animals were overdosed with isoflurane and perfused intracardially with saline followed by 4% paraformaldehyde. Brains were extracted and stored in 4% paraformaldehyde at 6 degrees C for at least 24 h. Approximately 72 h before slicing, brains were transferred into a 30% sucrose solution. The MEC was sliced along the sagittal plane to visualize tetrode tracks. Sections were mounted on gelatin-subbed glass slides and stained with cresyl violet.

Experimental design

One to two 20-min baseline (pre-injection) recording sessions were performed prior to drug or vehicle injection. After drug administration, recording sessions were performed up to 45 min in duration to ensure adequate coverage of the environment. This session began within 10 min following 8-OH-DPAT administration and 30 min post-diazepam injection. A 20-min recovery session was recorded 3–6 h postinjection and 24 h later, to confirm return to baseline activity. Multiple experiments, including medial septum infusion of different types of drugs in a separate experiment, were performed in a rat as long as a given grid cell could be well isolated; however, there was a minimum of 48 h between all drug and vehicle administrations. When single units of interest could no longer be isolated, tetrodes were moved down and screening for new cells of interest began again.

Drugs and drug administration

Drugs were administered systemically through intraperitoneal injection. Volume-matched vehicle controls were performed for systemic injections as well. The 5-HT1A receptor agonist, 8-OH-DPAT (Sigma), was mixed in sterile phosphate buffered saline to make a concentration of 100 μg/mL and administered at 75 μg/kg ($n = 6$ rats). The benzodiazepine, diazepam (Sigma), was mixed in DMSO to make a concentration of 1.0 mg/mL and administered at 1.0 mg/kg ($n = 7$ rats).

8-OH-DPAT

Effective doses of 8-OH-DPAT given via intraperitoneal injection reported in the literature range from 15 μg/kg up to 2.5 mg/kg (Klancnik et al., 1989; Coop et al., 1992; Warburton et al., 1997; Santucci and Shaw, 2003; Manuel-Apolinar and Meneses, 2004). Different doses were tested for this work (50, 75, 100, and 150 μg/kg; in two animals not used in this study and two that were), and 75 μg/kg was found to be the highest dose that could be given without disrupting ambulation in most cases. In reported administrations of this drug, injections were given within a range of 15 min to 30 min before the given experimental session began, in most cases. When tested and reported, peak effects were achieved 30 or 45 min post administration (Klancnik et al., 1989; Coop et al., 1992) but in both experiments, near maximum levels were reported 15 min postinjection. In this work, recordings typically began within 10 min postinjection.

Diazepam

Systemic administration of diazepam in rodents has been widely performed, with effects reported for amounts ranging from 1 mg/kg and up (Pellow et al., 1985; Dunn et al., 1989; Arolfo and Brioni, 1991; Brioni and Arolfo, 1992). In this work, 1 mg/kg was administered as this dose was commonly found in the literature and did not greatly affect ambulation in most cases. In most reported cases, diazepam injection preceded experimental testing by 30 min; so the same delay was utilized in the experiments presented here.

Analyses

Cluster cutting across sessions. After the completion of each recording session, single units were isolated using cluster cutting software (Offline Sorter, Plexon Inc.). Single units were distinguished using peak amplitude and principal components for each waveform. Stability of units was confirmed by tracking waveform profiles across the four leads of the tetrode and cluster position across recording sessions, comparing to the baseline session.

Measurement of theta rhythm and running speed. LFP activity was collected at 32 kHz and downsampled to 508 Hz. Downsampled LFP was filtered using a second order butterworth bandpass filter with cutoff frequencies of 6–10 Hz for theta band. Phase was estimated using the angle of the Hilbert transform of the filtered signal and used to estimate instantaneous frequency. Cycle-by-cycle frequency was calculated based on the peak-to-peak time; cycles with a calculated frequency outside of theta (6–10 Hz) were discounted. The LFP channel used for analyses was chosen on an animal-by-animal basis for each set of four recording sessions based on spectral properties from the baseline recording (Brandon et al., 2013). For each channel the spectrum of LFP power was found, the peak within theta range determined, and divided by the mean signal, giving the relative power within the theta band, which was also used for theta power analyses. The LFP channel was then chosen as the channel with maximum theta-to-noise ratio for each rat's baseline session. Theta frequency was calculated for 2.5 cm/s running speed bins and plotted for speeds ranging from 5 to 30 cm/s. Theta frequency from each rat's LFP signal was normalized to aid comparison between animals similar to Wells et al. (2013). In brief, the overall mean across all animals during the baseline recording session was calculated. A normalization factor was determined on an animal-by-animal basis as the mean difference in the animal's baseline signal from the population mean. This normalization factor was applied across all sessions for each animal, giving a normalized signal. This method accounts for a mean difference but not speed modulated difference, in theta frequency between animals.

A linear regression was performed on the normalized means across running speed bins from the rats within an experimental group (e.g. diazepam data) to determine the best linear fit to the data. From this, the intercept and slope of the linear relationship between theta frequency and running speed was determined and used for statistical analyses.

Measurement of single unit properties. Spatial rate maps were constructed for a given unit by taking the number of spikes in 3.6 cm by 3.6 cm spatial bins and dividing by the amount of time spent in that bin. Rate maps were smoothed using a 5×5 bin 2D-Gaussian kernel with a one-bin standard deviation. The spatial periodicity of grid cells was quantified with a "gridness" score and computed from the spatial autocorrelation of the smoothed rate maps (Brandon et al., 2011). In brief, to calculate the gridness score, "gridness 3" from Brandon et al. (2011), the center peak was removed from the autocorrelation and if present, the six surrounding peaks were found and cut out to make a donut. If the grid shape was elliptical, it was distorted to create a circle. The correlation was calculated for each 3 degree rotation of the donut to itself. The gridness score is the difference between the correlation at the minimum peak of 60 or 120 degrees and the maximum trough at 30, 90, or 150 degrees. The grid field spacing was determined from the spatial autocorrelation by calculating the average distance between the center of the middle and six surrounding peaks and checked manually to ensure the proper fields were being detected and measured. If the correct fields could not be accurately measured, those data were not used in the grid field spacing analysis (this left 24/40 grid cells suitable for this analysis).

Head direction firing properties of units were calculated by constructing a polar histogram of firing rates by head direction. Spikes were put into bins of 6 degrees and divided by the amount of time spent facing that direction. The mean resultant length and mean resultant angle of the directionality of spiking were then calculated.

The spatial information score reflects the degree to which a cell's spiking can be used to predict the animal's location. It was calculated as in Cacucci et al. (2007) and expressed in bits/spike. Correlations of the spatial rate maps for cells were calculated by finding the Pearson's correlation coefficient between the baseline rate map and the following sessions for a given cell.

Measurements of theta phase locking (mean resultant length, mean resultant angle) for single units were computed using the MATLAB CircStat toolbox (Berens, 2009) using the instantaneous theta phase for each spike time. Analysis of frequency and magnitude of theta rhythmic firing in single units was performed using a maximum likelihood estimation of a parametric model of the lags within the autocorrelation window (Climer et al., 2015). Two maximum likelihood estimation models were used to fit the lags of the autocorrelation of spike times. One model assumed no rhythmic firing (arrhythmic null hypothesis), while the second allowed for a modulatory effect of time since spike (i.e. rhythmicity). Comparing these two models gave an estimate and significance (p) value for the rhythmic firing of each neuron. Employing this maximum likelihood estimation approach offers a more

statistically rigorous and sensitive measure of theta rhythmic firing properties than the traditionally used theta index (Climer et al., 2015) and has been successfully implemented elsewhere as well (Hinman et al., 2016; Ebbesen et al., 2016).

Classification of cells. Single units were classified as grid cells, head direction cells, or spatially modulated non-grid cells. To determine gridness, head direction, and spatial information thresholds, shuffling was performed as in Bonnevie et al. (2013), for gridness 3, mean resultant length, and spatial information content, respectively. Briefly, the sequence of spikes from a given cell was time shifted along the rat's path by a random interval between 20 s and session length minus 20 s, with the end wrapped to the beginning. A single unit was deemed a given cell type if the value exceeded the 95th percentile of all shuffled permutations. The thresholds for gridness 3, mean resultant length, and spatial information were 0.2232, 0.2205, and 2.7591, respectively. Somewhat surprisingly, shuffling to determine the spatial information threshold resulted in a very high number, suggesting that even shuffled data often surpass the commonly used threshold of 0.5. Given this, and that few cells could therefore be classified as spatially modulated, analyses were limited to grid cells and head direction cells.

Data exclusion. If an animal did not cover at least 80% of the total number of position bins (3.6 cm $\times$ 3.6 cm) in the environment in the first 20 min of the recording session (length of most recordings) immediately following drug administration, that set of experiments were excluded from analyses (Bjerknes et al., 2014). This occurred in only two sets of recordings, both in the diazepam condition. This eliminated data from one rat and a repeated recording from another.

Histology was used to verify tetrode tracks to ensure they were positioned to record from the MEC area; in one animal the recording drive was positioned too anterior and data from that animal were excluded. Data from 10 animals were ultimately used in this study. Single units were used for analyses if they were stable enough to be recorded across the first three recording sessions (pre-injection, postinjection, and 3–6 h recovery), otherwise single unit data for that cell were excluded and not analyzed.

Statistical tests of significance. For LFP analyses, if a rat was used more than once in the same experimental condition, results were averaged so that each rat provided a single data point. In the 8-OH-DPAT condition 2 of the 6 rats contributed averaged LFP values from two sets of recordings each and for diazepam 1 of the 7 rats contributed averaged LFP values from 2 recordings. In the 8-OH-DPAT vehicle condition, out of 5 rats, 1 contributed averaged LFP values from 2 recordings and another rat contributed LFP values averaged from 3 recordings. In the diazepam vehicle condition, 1 out of the 5 rats contributed averaged LFP value from 2 recordings.

In all four experimental group baseline recordings (that is, baseline recordings before 8-OH-DPAT, diazepam, phosphate buffered saline (8-OH-DPAT vehicle), and DMSO (diazepam vehicle)), the linear regression analysis resulted in R values >0.98 and p values $<1e\text{-}6$ demonstrating a statistically significant relationship between theta frequency and running speed.

In order to examine drug effects on LFP theta frequency, values for the intercept and slope of the linear fit of the relationship between theta frequency across running speeds were calculated for the pre-injection and postinjection recording sessions for both drug and vehicle. The difference in the measure (i.e. intercept or slope) between the pre-injection and postinjection recording sessions was calculated for each rat (e.g. postinjection intercept minus pre-injection intercept). One-way ANOVAs were performed on these values to test for differences between drug and vehicle. To test for changes from pre- to postinjection within an experimental group (e.g. diazepam administrations), paired t-tests were performed between the pre-injection and postinjection values (e.g. intercept) to test for equal means. For most single unit analyses, one-way ANOVAs were performed to test for differences between drug and vehicle in the changes in the measure from pre- to postinjection recording sessions, similar to LFP.

Theta phase locking by grid cells was determined by looking at the phase of LFP theta for each cell spike and plotting across the "pass index" value (ranging from -1 to 1) of a rodent's movement through a grid field as in Climer et al. (2013). Theta phase locking of a cell's firing to LFP theta within a session was analyzed using a Rayleigh test for non-uniformity of circular data. A Watson-Williams multi-sample test for equal means was performed to test for changes in phase locking from the pre-injection recording session to the postinjection recording session. Only cells that showed significant phase locking ($p \leq 0.05$ for the Rayleigh test) were used for theta phase analyses.

For measures of single unit firing rhythmicity, a p value for each unit was determined by calculating a likelihood-ratio test to establish whether it was significantly rhythmic compared to the arrhythmic null hypothesis ($p \leq 0.05$) as in Climer et al. (2015). Only cells that were significantly rhythmic within theta range (6–12 Hz) during both the pre- and postinjection recording sessions were included in rhythmicity analyses (rhythmicity frequency and theta magnitude) (31/40 grid cells were significantly rhythmic in both recording sessions).

RESULTS

Effects of drug administration on LFP

Systemic injections of two neurochemically dissimilar anxiolytics, 8-OH-DPAT (5-HT1A receptor agonist) and diazepam (benzodiazepine), were performed to test the hypothesis that anxiolytic drugs decrease the frequency of LFP theta recorded in the MEC.

Overall, systemic administration of both 8-OH-DPAT and diazepam robustly decreased MEC theta frequency across running speeds, resembling results reported

previously in hippocampal recordings. As shown in Fig. 1, the intercept of the linear fit of LFP theta frequency across running speeds was reduced from pre-injection values after administration of both 8-OH-DPAT ($F(1,9) = 132.2$, $p < 0.001$) and diazepam ($F(1,11) = 9.45$, $p = 0.011$) compared to a lack of significant change after administration of vehicle. There was a small but significant decrease seen in the slope of the frequency-running speed relationship compared to pre-injection values after 8-OH-DPAT ($F(1,9) = 10.13$, $p = 0.011$) and diazepam ($F(1,11) = 8.47$, $p = 0.014$) compared to vehicle (Fig. 1).

In a separate examination of the change in slope between just the pre- to postinjection recording sessions (not comparing drug against vehicle), there was no significant change in slope after 8-OH-DPAT administration (paired $t(5) = -1.99$, $p = 0.10$). This suggests that the positive result from comparing 8-OH-DPAT to vehicle was likely from the slope increasing after the vehicle administration (paired $t(4) = 3.43$, $p = 0.03$), whereas after drug it did not. However, testing for differences between just the pre- and postinjection values for diazepam, there was a significant decrease in slope seen (paired $t(6) = -3.52$, $p = 0.01$). In fact, after diazepam administration, in some postinjection recording sessions the slope actually decreased enough that it became negative across running speeds ($n = 2$ of 8 postinjection recordings).

No changes in mean theta power were seen after 8-OH-DPAT ($F(1,8) = 2.39$, $p = 0.16$) or diazepam ($F(1,9) = 0.75$, $p = 0.41$) administration. Overall, in comparison with vehicle, median running speed was not affected by 8-OH-DPAT ($F(1,14) = 3.67$, $p = 0.08$) or diazepam ($F(1,13) = 1.51$, $p = 0.24$) administration, which suggests a decrease in running speed cannot account for the robust decrease seen in LFP theta frequency.

Effects of drug administration on single units

In order to test whether the decrease in LFP theta frequency after anxiolytic administration affected grid cell firing properties, two-sample t-tests were performed to test for changes between the pre- and postinjection recording sessions, comparing drug and vehicle. In total we recorded from and analyzed 40 grid cells across the experiments. For 8-OH-DPAT recordings we recorded a total of 10 grid cells through all stages of the drug condition (baseline, postdrug injection, and 3–6 h recovery session) and we recorded a total of 10 grid cells throughout all stages of the vehicle condition (baseline, post-vehicle injection, and 3–6 h recovery). For the diazepam condition we recorded 15 grid cells through all stages of the drug condition (baseline, postdrug injection, and 3–6 h recovery session) and we recorded a total of 5 grid cells through all stages of the vehicle condition (baseline, post-vehicle injection, and 3–6 h recovery).

The spatial periodicity and field distance of grid cell firing were unaffected by either drug. The spatially periodic firing, or gridness, of grid cells remained intact after administration of 8-OH-DPAT ($F(1,18) = 0.001$, $p = 0.97$) or diazepam ($F(1,18) = 0.26$, $p = 0.61$) (Fig. 2). Similarly, there were no significant differences in the distance between grid cell firing fields after 8-OH-DPAT ($F(1,11) = 3.13$, $p = 0.10$) or diazepam ($F(1,9) = 1.39$, $p = 0.27$) administration (Fig. 2). To address the possibility that grid cells of different sizes were unevenly

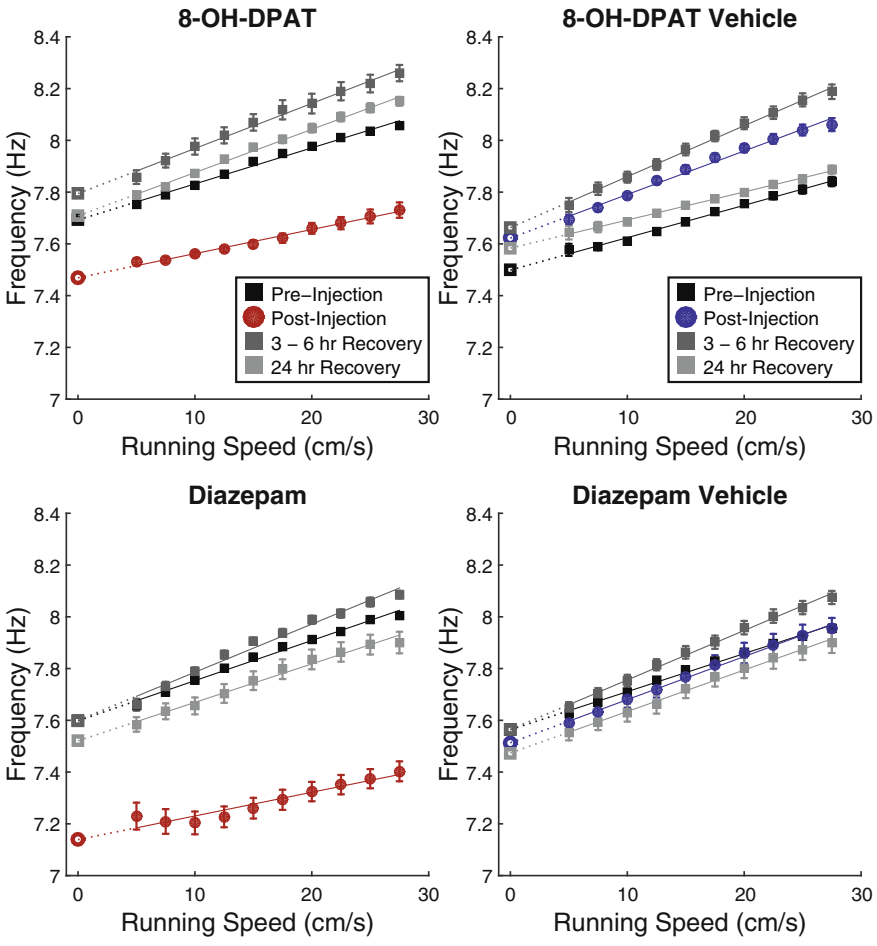

Fig. 1. Local field potential theta frequency across running speeds. Systemic administration of two different anxiolytic drugs robustly reduces local field potential theta frequency recorded in the medial entorhinal cortex. Local field potential theta frequency plotted across running speeds during pre-injection recording sessions (black squares) and after administration of anxiolytics (red circles; 8-OH-DPAT, top; diazepam, bottom) or their vehicles (blue circles; 8-OH-DPAT vehicle, top; diazepam vehicle, bottom). Recovery sessions are marked in gray (3–6 h recovery, dark gray; 24 h recovery, light gray).

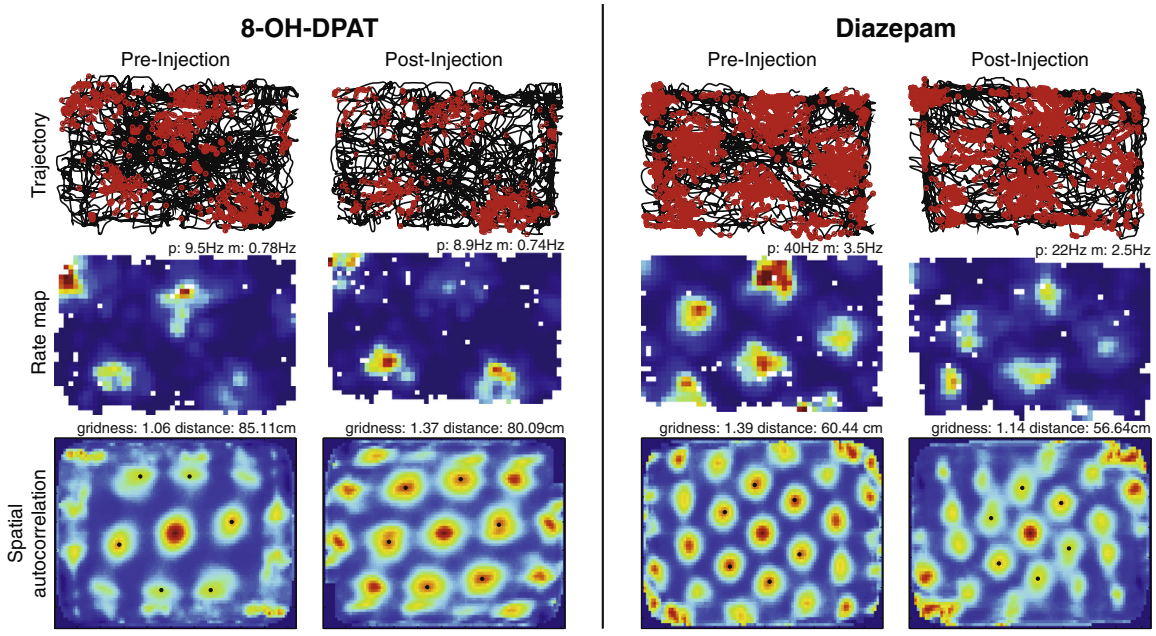

Fig. 2. Grid cell spatially modulated firing. Grid cell spatial periodicity and grid field scale remain intact after administration of two different anxiolytic drugs. Examples of two grid cells, one for each drug condition (8-OH-DPAT, left; diazepam, right). Top: trajectory plots with the animal's path in black and red dots overlaid with the position of the animal when each action potential occurred. Middle: rate map of grid cell firing. For each spatial bin, the number of action potentials occurring in that bin is divided by the amount of time spent in it and plotted as a heat map with warmer colors representing higher firing rates. p = peak firing rate; m = mean firing rate. Bottom: spatial autocorrelation of the rate map with the six surrounding fields used to detect distance marked with black dots. Gridness = gridness 3 score; distance = average distance between central and six outer nodes.

sampled across experimental groups, the difference in field distance as a proportion of field size from baseline to postinjection was examined as well and again, no significant differences were seen after 8-OH-DPAT ($F(1,11) = 3.02$, $p = 0.11$) or diazepam ($F(1,9) = 0.98$, $p = 0.35$) administration.

In contrast to the absence of a statistical effect on field spacing, the decrease in LFP theta frequency was accompanied by a significant decrease in the frequency of theta rhythmic firing by grid cells. Grid cell intrinsic rhythmicity frequency significantly decreased after both 8-OH-DPAT ($F(1,17) = 18.20$, $p < 0.001$) and diazepam ($F(1,10) = 15.19$, $p = 0.003$) administration (Fig. 3). Theta magnitude, or the degree to which a cell's firing is theta modulated, was unaffected by either 8-OH-DPAT ($F(1,17) = 0.24$, $p = 0.63$) or diazepam ($F(1,10) = 0.55$, $p = 0.48$) administration (Fig. 3).

Apart from this significant change in the frequency of the rhythmicity found in grid cell firing, no other significant differences were seen in single unit firing properties after 8-OH-DPAT or diazepam administration. No effect was found on grid cell firing rate after 8-OH-DPAT ($F(1,18) = 0.02$, $p = 0.89$) or diazepam ($F(18) = 0.06$, $p = 0.81$) administration. Examining the conjunctive (grid and head direction modulated) cells, no changes in the mean resultant length of directional firing were found after administration of 8-OH-DPAT ($F(1,7) = 0.48$, $p = 0.51$) or diazepam ($F(1,9) = 0.61$, $p = 0.45$).

Of grid cells that were significantly phase locked in their firing to LFP theta oscillations during the pre-injection recording (37 of 40 total grid cell recordings), all of them remained significantly phase locked after 8-OH-DPAT ($n = 10$) and diazepam ($n = 13$) administration, along with after 8-OH-DPAT vehicle ($n = 10$) and diazepam vehicle ($n = 4$) (Fig. 4).

No significant differences were found in the change in the mean resultant length of phase locking from the pre- to postinjection recording sessions after drug compared to vehicle for 8-OH-DPAT ($F(1,18) = 0.67$, $p = 0.42$) or diazepam ($F(1,15) = 0.16$, $p = 0.70$) administration (Fig. 5). The preferred phase of LFP theta locking (mean resultant angle) also remained the same after drug administration compared to vehicle for 8-OH-DPAT ($F(1,18) = 0.009$, $p = 0.93$) and diazepam ($F(1,15) = 0.07$, $p = 0.79$) administration (Fig. 5).

Given that head direction cells are known to be theta rhythmic as well, we next looked at whether the frequency of their theta rhythmic firing also decreased in concert with the decrease in LFP theta frequency and in grid cell rhythmic firing frequency. We found that after 8-OH-DPAT administration compared to vehicle, the decrease in theta frequency of the rhythmic firing of head direction cells did not reach significance ($F(1,9) = 4.38$, $p = 0.07$), though after diazepam administration there was a significant decrease in the frequency of theta rhythmic firing by head direction cells ($F(1,12) = 98.62$, $p < 0.001$).

DISCUSSION

These data show that systemic administration of both a serotonergic anxiolytic and benzodiazepine anxiolytic

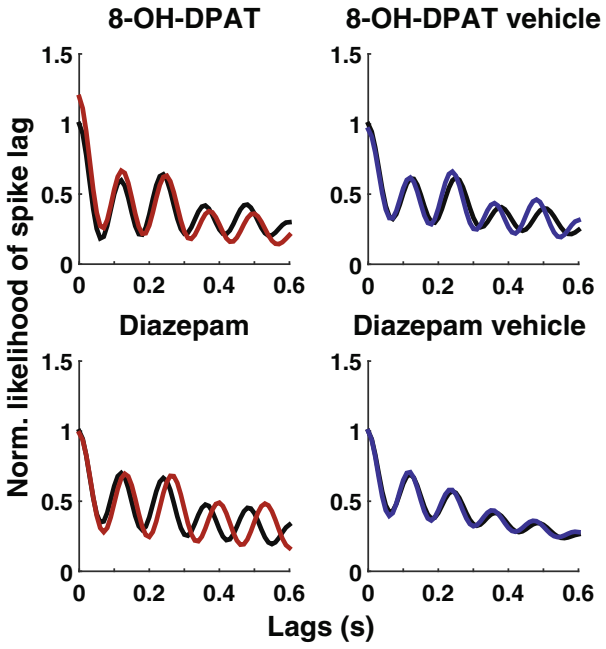

Fig. 3. Grid cell intrinsic rhythmicity frequency and magnitude of theta modulation. A parametric rhythmicity distribution of the firing of a given grid cell was calculated for each recording session, yielding the likelihood of a spike lag, given it occurred within 0.6 s of another spike. The group average of model parameters during baseline and postinjection recording sessions were normalized to the maximum likelihood value during baseline and plotted above. Grid cell rhythmicity shows a significant slowing of frequency (lags increase) after anxiolytic administration. Rhythmicity measures plotted include frequency (seen as left or right shifts), rhythmicity magnitude (amplitude of line), and falloff (decrease in amplitude with increasing lags) as in Climer et al. (2015); the only significant change is in frequency. Left: Mean grid cell rhythmicity for grid cells before injection of drug (black line) or after anxiolytic administration (red). Right: Mean grid cell rhythmicity for grid cells before injection of vehicle (black) or after vehicle administration (blue). Note the decrease in rhythmicity frequency (increase in lag) for both anxiolytic drugs, the increase in frequency (decrease in lag) for 8-OH-DPAT vehicle, and no change in frequency for diazepam vehicle match the effects seen on the local field potential. (For interpretation of the references to color in this figure legend, the reader is referred to the web version of this article.)

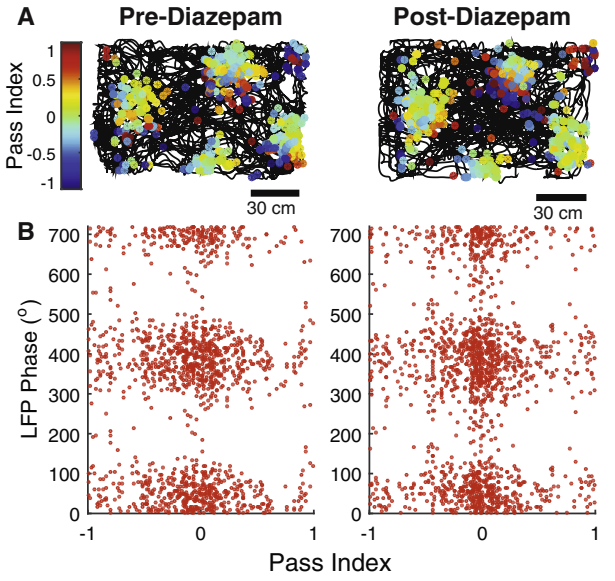

Fig. 4. Theta phase locking of grid cells through field passes. Example of consistent phase locking of grid cell firing to local field potential theta phase before and after anxiolytic administration. (A) Trajectory plot of the animal's movement (black lines) with circles marking the animal's position when the recorded cell fired an action potential. The color of the circle corresponds to the pass index value with cooler colors representing the rodent entering the grid field and warmer colors indicating exits for the given pass. (B) The local field potential phase of when the cell fired is plotted across the pass index indicating that regardless of how far along in the pass through the field the animal is, firing is locked to approximately the same phase of local field potential theta, both during the pre-injection (left) and postinjection (right) recording sessions.

robustly decreased theta frequency found in the LFP recorded in the MEC. Specifically, both the serotonergic agonist 8-OH-DPAT and the benzodiazepine diazepam greatly decreased the intercept of the linear fit to the plot of theta frequency across running speeds. In Fig. 1, this appears as a systematic decrease in frequency after drug injection across the full range of different running speeds. These results strongly corroborate the previously reported effects of anxiolytics on hippocampal LFP theta (Wells et al., 2013), expanding the detection of this systematic effect to a new structure, the MEC.

Surprisingly, based on past evidence of anxiolytics solely affecting the intercept, and not the slope, of the relationship between theta frequency across running speeds (Wells et al., 2013), we did see a small but significant decrease in slope after administration of either drug compared to its vehicle. However, when looking at the change within a drug group, and not accounting for change occurring during control experiments, no change was seen between pre- and postinjection of 8-OH-DPAT. In fact, an increase in slope was seen after 8-OH-DPAT vehicle administration, which could be due to a same day repeated-exposure effect on slope reported elsewhere (Newman et al., 2013; Wells et al., 2013). However, there was a significant decrease in slope after diazepam administration and in some recording sessions the slope was negative across running speeds. However even when this occurred, no changes in gridness or spacing were seen, despite this being predicted to be the case based on previous experimental results (Barry et al., 2007; Newman et al., 2013, 2014). This could be because the overall change in slope was actually quite small in comparison with the change that occurs in novel environment experiments (Barry et al., 2007) so even if there was a change in grid scale it might have been too small to detect. Diazepam administration is widely known to produce anterograde amnesia (Ghoneim and Mewaldt, 1975; Lister, 1985; Thiébot, 1985), though it is unlikely the effects on slope seen here are due to that since the effect on memory would not manifest until the recovery recording session.

Previous studies have shown a consistent increase during control conditions in the slope of LFP theta frequency across running speeds over multiple recording sessions on the same day in a familiar environment (Jeewajee et al., 2008b; Newman et al., 2013; Wells et al., 2013). There was a significant increase in slope during the postinjection recording session after

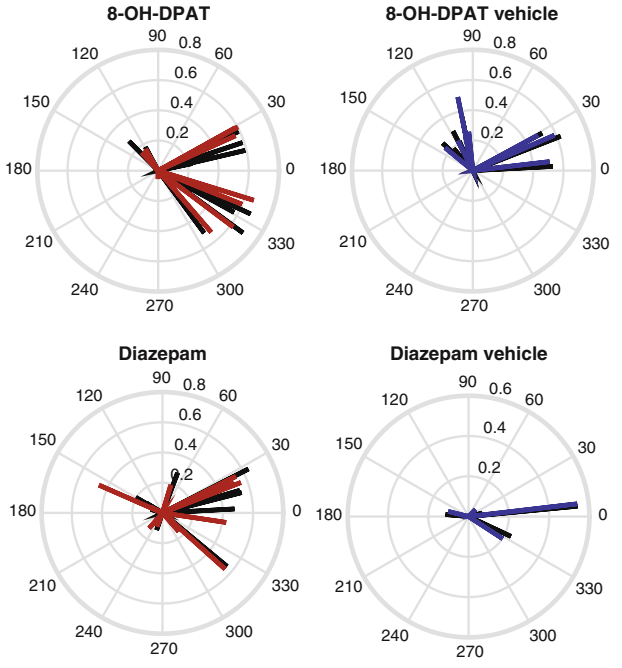

Fig. 5. Phase preference and strength of grid cell firing to local field potential theta. The mean resultant length and mean resultant angle of grid cell phase locking to local field potential theta remain intact from pre- to postinjection recordings for all drugs and their vehicles. Each line represents the phase locking measure of a grid cell during the pre-injection (black lines) and postinjection (colored lines) recording sessions. Note the consistent clustering of pairs and groups of the black and colored lines to each other.

8-OH-DPAT vehicle administration, though no increase was seen after diazepam vehicle administration. It does appear that at least for the first recovery recording session (3–6 h postinjection), the slope may have increased compared to the pre-injection recording session regardless of the experimental condition (drug or vehicle), suggesting an increase in slope due to a same-day repeated exposure could be occurring (Fig. 1, dark gray: 3–6 h recovery).

We did observe a significant increase in the intercept of the relationship between theta frequency and running speed after PBS vehicle administration (the vehicle for 8-OH-DPAT), though similar to slope, this was not seen after DMSO vehicle administration (the vehicle for diazepam) (Fig. 1). It is unclear whether this is also related to a same-day repeated exposure increase in theta frequency or due to something different.

Overall, the intercept of the relationship between theta frequency and running speed was significantly altered by both of the anxiolytic drugs and possibly with repeated same-day exposures, but no changes were seen in grid field spacing. These results lend support to the prediction by Burgess (Burgess, 2008) that a decrease in theta frequency via the intercept of the relationship between theta frequency and running speed is not sufficient to produce changes in grid field spacing. Furthermore, theta power was unaffected after administration of either anxiolytic. This is in line with what was reported in the hippocampus after systemic injection of similar anxiolytics as well (Wells et al., 2013).

Consistent with the effects observed in the LFP, we found a significant change in the frequency of grid cell rhythmic firing after 8-OH-DPAT or diazepam administration (Fig. 3) and a significant change in the theta rhythmic firing of head direction cells after diazepam injection. In contrast to this significant effect on rhythmicity, no other significant changes in grid cell firing properties were observed. No changes were seen in grid cell firing rates after administration of either drug, similar to what was reported in principal cells in the hippocampus (Wells et al., 2013). This finding highlights the resiliency of grid cells in general to local perturbations in LFP frequency and the importance of the inputs the cells receive from other areas that pass on different information.

The significant decrease found in the frequency of the rhythmic firing by grid cells after anxiolytic administration likely reflects the maintenance of grid cell phase locking to LFP theta phase. As LFP theta frequency decreased, the firing slowed to remain locked to a constant preferred phase, resulting in a decrease in the grid cell's rhythmicity frequency. This is evident in the finding that all phase locked grid cells remained significantly phase locked after drug administration and there was no change in the strength or preferred phase of their selectivity (Fig. 5). The decrease in intrinsic frequency in head direction cells after 8-OH-DPAT administration did not reach significance, though there was a significant decrease after diazepam injection. This could be due to the smaller decrease in LFP theta frequency after 8-OH-DPAT administration compared to diazepam so if there was a slowing in the rhythmicity in head direction cells it might have been more difficult to detect (Figs. 1 and 3). This overall maintenance of grid cell phase locking to LFP theta, despite induced perturbations in frequency of the oscillation, may be necessary to maintain accurate internal spatial representations and updating during navigation.

The limits of histology make it difficult to pinpoint exactly what layer the grid cells were recorded from due to the approach of the tetrodes traveling through deeper to superficial layers and that they were advanced after grid cell recordings with the goal of recording more. However, based on the direction of approach used here, the number of conjunctive grid-by-head-direction cells, and the lack of phase precession in cell firing, this suggests it is very likely that the recordings were from cells in deeper layers of the MEC (Sargolini et al., 2006; Hafting et al., 2008). Further studies could examine the response of grid cells located more superficially, especially in terms of phase precession.

At first glance, the robust decrease in the intercept of theta frequency plotted across running speeds and lack of change in grid scale seems to confirm Burgess' (2008) predictions based on the OIM. However, the finding that a concurrent decrease in slope occurred without a change in grid scale complicates interpretation. It might be that the underlying mechanisms producing this decrease in slope differ from what is required to produce grid scale changes. Involvement of acetylcholine might be necessary for an effect of theta frequency changes on grid scale, whether through increases in grid scale and

decrease in slope in response to novelty (Barry et al., 2007), or in the complete disruption of grid scale and a flattening of slope when anticholinergics are administered systemically (Newman et al., 2013, 2014). Just as the link between changes in grid field scale and theta frequency is not as simple as a global reduction in frequency but rather can be dissociated through intercept and slope of theta frequency across running speeds, changes to the slope might be dissociated further as well.

Involvement of the entorhinal cortex in anxiety has been noted before, such as in the case of pain modulation by anxiety (Ploghaus et al., 2001), though research has generally focused on the contributions of other regions of the hippocampal formation, namely the hippocampus. The hippocampus has previously been implicated in anxiety (Deacon et al., 2002; Bannerman et al., 2004) and specifically, ventral hippocampal lesions reduce anxiety while sparing spatial learning in rats (Kjelstrup et al., 2002; Bannerman et al., 2003; Pentkowski et al., 2006). However, anxiolytic drugs have widely been shown to produce memory deficits (Ghoneim and Mewaldt, 1975), including in spatial learning (McNaughton and Morris, 1987, 1992; Arolfo and Brioni, 1991; Carli and Samanin, 1992), though the results presented here demonstrate these spatial memory impairments are not caused by disruption of the spatially modulated firing of grid cells. Anxiolytic effects on hippocampal theta rhythm frequency have been extensively studied for decades (for review see McNaughton et al. (2007)). Despite differing mechanisms of action, different types of anxiolytic drugs all produce similar decreases in hippocampal theta frequency (McNaughton and Coop, 1991), suggesting a complex interplay of systems involved in anxiolytic action, which outwardly manifests as a recordable change in theta frequency. The results described here add to this, expanding the detection of effects of this class of drugs to a novel structure, the entorhinal cortex.

Acknowledgements—The authors would like to thank Win Gillis and Anna Stopa for help in data collection and histology, lab technicians Tyler Ware, Elijah Petter, Eri Yamaguchi, Ron DiTullio, and Britahny Baskin for help constructing drives and maintaining the laboratory, and Mark Brandon for help in implantation surgeries and ongoing technical help.

Experiments were performed by CKM, data analysis was done by CKM and GWC, and the manuscript was written by CKM and MEH.

Funding—This work was supported by National Institute of Mental Health R01 MH60013, R01 MH61492, and Office of Naval Research MURI award N00014-10-1-0936.

Conflict of interest—The authors declare no conflicts of interest.

REFERENCES

Alonso A, García-Austt E (1987) Neuronal sources of theta rhythm in the entorhinal cortex of the rat. I. Laminar distribution of theta field potentials. Exp Brain Res 67:493–501.

Arolfo MP, Brioni JD (1991) Diazepam impairs place learning in the Morris water maze. Behav Neural Biol 55:131–136.

Bannerman DM, Grubb M, Deacon RMJ, Yee BK, Feldon J, Rawlins JNP (2003) Ventral hippocampal lesions affect anxiety but not spatial learning. Behav Brain Res 139:197–213.

Bannerman DM, Rawlins JNP, McHugh SB, Deacon RMJ, Yee BK, Bast T, Zhang WN, Pothuizen HHJ, Feldon J (2004) Regional dissociations within the hippocampus - memory and anxiety. Neurosci Biobehav Rev 28:273–283.

Barry C, Ginzberg LL, O'Keefe J, Burgess N (2012) Grid cell firing patterns signal environmental novelty by expansion. Proc Natl Acad Sci USA 109:17687–17692.

Barry C, Hayman R, Burgess N, Jeffery KJ (2007) Experience-dependent rescaling of entorhinal grids. Nat Neurosci 10:682–684.

Berens P (2009) CircStat: a MATLAB toolbox for circular statistics. J Stat Softw 31.

Bjerknes TL, Moser EI, Moser M-B (2014) Representation of geometric borders in the developing rat. Neuron 7:1–8.

Bland BH (1986) The physiology and pharmacology of hippocampal formation theta rhythms. Prog Neurobiol 26:1–54.

Boccara CN, Sargolini F, Thoresen VH, Solstad T, Witter MP, Moser EI, Moser M-B (2010) Grid cells in pre- and parasubiculum. Nat Neurosci 13:987–994.

Bonnevie T, Dunn B, Fyhn M, Hafting T, Derdikman D, Kubie JL, Roudi Y, Moser EI, Moser M-B (2013) Grid cells require excitatory drive from the hippocampus. Nat Neurosci 16:309–317.

Brandon MP, Bogaard AR, Schultheiss NW, Hasselmo ME (2013) Segregation of cortical head direction cell assemblies on alternating theta cycles. Nat Neurosci 16:739–748.

Brandon MP, Bogaard AR, Libby CP, Connerney MA, Gupta K, Hasselmo ME (2011) Reduction of theta rhythm dissociates grid cell spatial periodicity from directional tuning. Science 332:595–599.

Brioni JD, Arolfo MP (1992) Diazepam impairs retention of spatial information without affecting retrieval or cue learning. Pharmacol Biochem Behav 41:1–5.

Brun VH, Solstad T, Kjelstrup KB, Fyhn M, Witter MP, Moser EI, Moser M-B (2008) Progressive increase in grid scale from dorsal to ventral medial entorhinal cortex. Hippocampus 18:1200–1212.

Burgess N (2008) Grid cells and theta as oscillatory interference: theory and predictions. Hippocampus 18:1157–1174.

Cacucci F, Wills TJ, Lever C, Giese KP, O'Keefe J (2007) Experience-dependent increase in CA1 place cell spatial information, but not spatial reproducibility, is dependent on the autophosphorylation of the alpha-isoform of the calcium/calmodulin-dependent protein kinase II. J Neurosci 27:7854–7859.

Carli M, Samanin R (1992) 8-Hydroxy-2-(di-n-propylamino)tetralin impairs spatial learning in a water maze: role of postsynaptic 5-HT1A receptors. Br J Pharmacol 105:720–726.

Climer JR, DiTullio R, Newman EL, Hasselmo ME, Eden UT (2015) Examination of rhythmicity of extracellularly recorded neurons in the entorhinal cortex. Hippocampus 25:460–473.

Climer JR, Newman EL, Hasselmo ME (2013) Phase coding by grid cells in unconstrained environments: two-dimensional phase precession. Eur J Neurosci 38:2526–2541.

Coop CF, McNaughton N (1991) Buspirone affects hippocampal rhythmical slow activity through serotonin1A rather than dopamine D2 receptors. Neuroscience 40:169–174.

Coop CF, McNaughton N, Scott DJ (1992) Pindolol antagonizes the effects on hippocampal rhythmical slow activity of clonidine, baclofen and 8-OH-DPAT, but not chlordiazepoxide and sodium amylobarbitone. Neuroscience 46:83–90.

Deacon RMJ, Bannerman DM, Rawlins JNP (2002) Anxiolytic effects of cytotoxic hippocampal lesions in rats. Behav Neurosci 116:494–497.

Dunn RW, Corbett R, Fielding S (1989) Effects of 5-HT1A receptor agonists and NMDA receptor antagonists in the social interaction test and the elevated plus maze. Eur J Pharmacol 169:1–10.

Ebbesen CL, Reifenstein ET, Tang Q, Burgalossi A, Ray S, Schreiber S, Kempter R, Brecht M (2016) Cell type-specific differences in spike timing and spike shape in the rat parasubiculum and superficial medial entorhinal cortex. Cell Reports 16:1005–1015.
Fyhn M, Molden S, Witter MP, Moser EI, Moser M-B (2004) Spatial representation in the entorhinal cortex. Science 305:1258–1264.
Ghoneim MM, Mewaldt SP (1975) Effects of diazepam and scopolamine on storage, retrieval and organizational processes in memory. Psychopharmacologia 44:257–262.
Giocomo LM, Zilli EA, Fransén E, Hasselmo ME (2007) Temporal frequency of subthreshold oscillations scales with entorhinal grid cell field spacing. Science 315:1719–1722.
Green JD, Arduini AA (1954) Hippocampal Electrical Activity in Arousal. J Neurophysiol 17:533–557.
Hafting T, Fyhn M, Bonnevie T, Moser M-B, Moser EI (2008) Hippocampus-independent phase precession in entorhinal grid cells. Nature 453:1248–1252.
Hafting T, Fyhn M, Molden S, Moser M-B, Moser EI (2005) Microstructure of a spatial map in the entorhinal cortex. Nature 436:801–806.
Hinman JR, Brandon MP, Climer JR, Chapman GW, Hasselmo ME (2016) Multiple running speed signals in medial entorhinal cortex. Neuron 91:666–679.
Jeewajee A, Barry C, O'Keefe J, Burgess N (2008a) Grid cells and theta as oscillatory interference: electrophysiological data from freely moving rats. Hippocampus 18:1175–1185.
Jeewajee A, Lever C, Burton S, O'Keefe J, Burgess N (2008b) Environmental novelty is signaled by reduction of the hippocampal theta frequency. Hippocampus 18:340–348.
Kjelstrup KG, Tuvnes FA, Steffenach H-A, Murison R, Moser EI, Moser M-B (2002) Reduced fear expression after lesions of the ventral hippocampus. Proc Natl Acad Sci USA 99:10825–10830.
Klancnik JM, Baimbridge KG, Phillips AG (1989) Increased population spike amplitude in the dentate gyrus following systemic administration of 5-hydroxytryptophan or 8-hydroxy-2-(di-n-propylamino)tetralin. Brain Res 505:145–148.
Lister RG (1985) The amnesic action of benzodiazepines in man. Neurosci Biobehav Rev 9:87–94.
Manuel-Apolinar L, Meneses A (2004) 8-OH-DPAT facilitated memory consolidation and increased hippocampal and cortical cAMP production. Behav Brain Res 148:179–184.
McNaughton N, Coop CF (1991) Neurochemically dissimilar anxiolytic drugs have common effects on hippocampal rhythmic slow activity. Neuropharmacology 30:855–863.
McNaughton N, Kocsis B, Hajós M (2007) Elicited hippocampal theta rhythm: a screen for anxiolytic and procognitive drugs through changes in hippocampal function? Behav Pharmacol 18:329–346.
McNaughton N, Morris RGM (1992) Buspirone produces a dose-related impairment in spatial navigation. Pharmacol Biochem Behav 43:167–171.
McNaughton N, Morris RGM (1987) Chlordiazepoxide, an anxiolytic benzodiazepine, impairs place navigation in rats. Behav Brain Res 24:39–46.
Mitchell S, Ranck JB (1980) Generation of theta rhythm in medial entorhinal cortex of freely moving rats. Brain Res 189:49–66.
Newman EL, Climer JR, Hasselmo ME (2014) Grid cell spatial tuning reduced following systemic muscarinic receptor blockade. Hippocampus 24:643–655.
Newman EL, Gillet SN, Climer JR, Hasselmo ME (2013) Cholinergic blockade reduces theta-gamma phase amplitude coupling and speed modulation of theta frequency consistent with behavioral effects on encoding. J Neurosci 33:19635–19646.
O'Keefe J, Burgess N (2005) Dual phase and rate coding in hippocampal place cells: theoretical significance and relationship to entorhinal grid cells. Hippocampus 15:853–866.
Pellow S, Chopin P, File SE, Briley M (1985) Validation of open : closed arm entries in an elevated plus-maze as a measure of anxiety in the rat. J Neurosci Methods 14:149–167.
Pentkowski NS, Blanchard DC, Lever C, Litvin Y, Blanchard RJ (2006) Effects of lesions to the dorsal and ventral hippocampus on defensive behaviors in rats. Eur J Neurosci 23:2185–2196.
Ploghaus A, Narain C, Beckmann CF, Clare S, Bantick S, Wise R, Matthews PM, Rawlins JN, Tracey I (2001) Exacerbation of pain by anxiety is associated with activity in a hippocampal network. J Neurosci 21:9896–9903.
Santucci AC, Shaw C (2003) Peripheral 8-OH-DPAT and scopolamine infused into the frontal cortex produce passive avoidance retention impairments in rats. Neurobiol Learn Mem 79:136–141.
Sargolini F, Fyhn M, Hafting T, McNaughton BL, Witter MP, Moser M-B, Moser EI (2006) Conjunctive representation of position, direction, and velocity in entorhinal cortex. Science 312:758–762.
Stensola H, Stensola T, Solstad T, Froland K, Moser M-B, Moser EI (2012) The entorhinal map is discretized. Nature 492:72–78.
Taube JS, Muller RU, Ranck JB (1990) Head-direction cells recorded from the postsubiculum in freely moving rats. I. Description and quantitative analysis. J Neurosci 10:420–435.
Thiébot MH (1985) Some evidence for amnesic-like effects of benzodiazepines in animals. Neurosci. Biobehav. Rev. 9:95–100.
Vanderwolf C (1969) Hippocampal electrical activity and voluntary movement in the rat. Electroencephalogr Clin Neurophysiol 26:407–418.
Warburton EC, Harrison AA, Robbins TW, Everitt BJ (1997) Contrasting effects of systemic and intracerebral infusions of the 5-HT(1A) receptor agonist 8-OH-DPAT on spatial short-term working memory in rats. Behav Brain Res 84:247–258.
Wells CE, Amos DP, Jeewajee A, Douchamps V, Rodgers J, O'Keefe J, Burgess N, Lever C (2013) Novelty and anxiolytic drugs dissociate two components of hippocampal theta in behaving rats. J Neurosci 33:8650–8667.

(Received 28 April 2017, Accepted 30 August 2017)
(Available online 8 September 2017)